

General Disclaimer

One or more of the Following Statements may affect this Document

- This document has been reproduced from the best copy furnished by the organizational source. It is being released in the interest of making available as much information as possible.
- This document may contain data, which exceeds the sheet parameters. It was furnished in this condition by the organizational source and is the best copy available.
- This document may contain tone-on-tone or color graphs, charts and/or pictures, which have been reproduced in black and white.
- This document is paginated as submitted by the original source.
- Portions of this document are not fully legible due to the historical nature of some of the material. However, it is the best reproduction available from the original submission.

(NASA-TM-85079) THE MXB1916-053/4U1915-05:
BURST PROPERTIES AND CONSTRAINTS ON A 50
MINUTE BINARY SECONDARY (NASA) 40 p
HC A03/MF A01

N83-34862

CSSL 03A

Unclas
G3/89 4 1988



Technical Memorandum 85079

MXB1916-053/4U1915-05: BURST PROPERTIES AND CONSTRAINTS ON A 50 MINUTE BINARY SECONDARY

J.H. Swank
R.E. Taam
N.E. White

August 1983



National Aeronautics and
Space Administration

Goddard Space Flight Center
Greenbelt, Maryland 20771

**MXB1916-053/4U1915-05: BURST PROPERTIES
AND CONSTRAINTS ON A 50 MINUTE BINARY SECONDARY**

J.H. Swank

**Laboratory for High Energy Astrophysics
NASA/Goddard Space Flight Center**

R.E. Taam¹

**Department of Physics and Astronomy
Northwestern University**

and

N.E. White²

**Laboratory for High Energy Astrophysics
NASA/Goddard Space Flight Center**

¹Research supported in part by NSF AST-8109826

²Also Dept. of Physics & Astronomy, Univ. of Maryland

ABSTRACT

Results are presented from OSO-8 and HEAO-1 A2 observations of 34 bursts from the X-ray burster MXB1916-053/4U1915-05 recently discovered to show a 50 minute binary period. While 11 bursts previously reported all had similar light curves, 22 observed two years later show a factor of 3 range of peak fluxes and decay times between 3 and 20 s. Recurrence times between successive bursts vary between 3 and 6 hours. We derive a ratio of steady flux to average burst flux of ~ 120 . A burst observed with the HEAO-1 A2 experiment showed an initial temperature rise to a peak black body temperature of ~ 3 keV followed by the cooling typical of type I bursts. The burst was unusual in that the apparent projected size of a blackbody source increased by a factor of 3 during the cooling phase.

A 50 minute binary period allows many different types of mass losing star. We attempt to use the characteristics of the burster to discriminate between them and to determine if for some solution, consistent with the burst properties, the angular momentum loss through gravitational radiation can drive the mass transfer. Results of thermonuclear flash models of bursts imply the secondary is not hydrogen exhausted and that the mass transfer rate is greater than gravitational radiation can drive for any of the conventional models that have, to date, been worked out in detail. If the peak burst luminosities are typical of those of other bursters (assumed to emit isotropically) the implied distance and the steady flux also give a high mass transfer. A composite model for the secondary is marginally consistent within a factor of 2. Several mechanisms which could promote higher rates of mass transfer are discussed.

I. INTRODUCTION

White and Swank (1982, hereafter Paper I) and Walter et al. (1982) independently reported the discovery of absorption dips in the X-ray flux from 4U1915-05, recurrent with a period of ~ 50 minutes. Both papers gave strong arguments in favor of interpreting the periodic phenomenon as the orbital period of the system. 4U1915-05 = MXB 1916-053 is a source of type I X-ray bursts, each lasting ~ 10 s, with a recurrence time of several hours (Becker et al. 1977; Lewin, Hoffman and Doty 1977). This is the first X-ray burster to show a confirmed X-ray periodicity. As discussed in Paper I and by Walter et al. (1982) there are jitters and irregularities in the dips, so that they are not as good a clock as partial eclipses by a companion might be expected to be, and a picture was developed analogous to that of cataclysmic variables in which a gas stream from the secondary impacts an accretion disk in a turbulent "hot spot", and the thickened region of the disk occults the X-ray source.

The 50 minute orbital period of MXB 1916-053 is very close to the 46 minute orbital period of the 7s X-ray pulsar 4U1626-67, the orbit of which was identified from optical observations of X-ray pulsations reprocessed on the binary companion (Middleditch et al. 1981). Failure to find any Doppler shift in the X-ray pulses of 4U1626-67 and accumulating optical identifications of faint counterparts to this and many other non-pulsing, non-eclipsing sources led Joss and Rappaport (1979), prior to the discovery by Middleditch et al. (1981), to propose that the secondary mass should be $\lesssim 0.5 M_{\odot}$ in 4U1626-67 and in the bright galactic center and globular cluster sources. This mass is low enough that evolutionary mechanisms would lead in reasonable lifetimes to very compact binaries in which the secondary might have become degenerate (Joss, Avni, and Rappaport 1978). Some of these sources (Cyg X-2, Sco X-1,

4U0614+09, Aql X-1) may have periods on the order of days (Cowley, Crampton and Hutchings 1979; Cowley and Crampton 1975; Marshall and Millit 1981; Watson 1976). However, recent identifications of $\sim 5^h$ periods for 4U1822-37 and 4U2129-47 (Mason et al. 1980; Thorstensen et al. 1979) and $\sim 4^h$ periods for 4U1636-53 and 4U1735-44 (Pedersen, van Paradijs and Lewin 1982; McClintock and Petro 1981) imply secondaries that would populate the upper end of the predicted range ($\sim 0.5 M_{\odot}$). Evolution is expected to lead to shorter periods for these systems and MXB1916-053 and 4U1626-67 may be examples of this.

For orbital periods less than a few hours it has been postulated that gravitational radiation (GR) dominates the angular momentum losses that cause the orbits to decay (Faulkner 1971; Paczynski 1967). The limit on how compact a system will become depends on the secondary's original composition and its history. Orbital periods < 50 min are much shorter than the limits recently calculated for a secondary with standard abundances (Paczynski 1981; Paczynski and Sienkiewicz 1981; Rappaport, Joss and Webbink 1982, hereafter RJW; Whyte and Eggleton 1981). Both paper I and Walter et al. (1982) discussed possible types of unevolved stars that could "fit into" a 50 minute binary with a $1.4 M_{\odot}$ neutron star. A consistent picture for any of these or other possibilities was not addressed, although it has been pointed out (Kieboom and Verbunt 1981; RJW) that compact binaries with main sequence secondaries could not evolve to the most luminous X-ray binaries with mass transfer driven by GR alone.

While X-ray bursts are not "standard candles" in the sense of having unique peak luminosities (see Lewin 1982 a,b for references and discussion) they still potentially offer important information on the nature of the secondary that is not available for many bulge sources. A range of observed peak luminosities is deduced from sources which can reasonably be assumed to cluster close to the galactic center (Inoue et al. 1980; van Paradijs 1981).

Although the emission may be modified by a scattering dominated atmosphere (estimates have been given by Swank, Eardley and Serlemitsos 1979; van Paradijs, Rybicki and Lamb 1979; van Paradijs 1982), the spectra can be reasonably well described by a blackbody form and a range of effective projected sizes for the sources has been determined. The bursts can be interpreted within the framework of the thermonuclear flash model of X-ray bursts to estimate the mass transfer rate and deduce the composition of the accreted material, and hence test the consistency of the current evolutionary models.

In the next section we present new observational data of X-ray bursts emitted from MXB1916-053. In §III we deduce the parameters of the system from the X-ray bursts. Theoretical considerations based on binary star evolution will be described in §IV, and used with thermonuclear flash theory to restrict the parameters of the system in §V. Finally, we discuss some suggested avenues toward a self-consistent picture.

II. BURST OBSERVATIONS

The observations were made with the Goddard Space Flight Center proportional counter detectors on the OSO-8 and HEAO-1 satellites and the different sensitivities and observational constraints of the two experiments allow different aspects of the burst properties to be investigated. MXB1916-053 was burst active during the several days of OSO-8 observations in March 1976 and March 1978. Both observations provide measures of the recurrence times and steady flux, along with limited indications of burst properties such as peak luminosities, temperatures, rise and decay times and burst energies. Only one short 4 hour pointed observation with the much larger area experiment on HEAO-1 A2 was made, but one burst was observed; the data on this one burst provides substantially more information about the

spectral evolution than is possible with the OSO-8 data. While the information available from OSO-8 on individual bursts is limited, these observations do give information on the range of light curves and spectral properties. Comparison of results indicates that the one burst observed with HEAO-1 A2 was similar to some of those observed with OSO-8.

A. Recurrence Time

Figure 1 shows both the time that elapsed between bursts and the average steady flux from the source as a function of time for all the OSO-8 observations. Gaps in the data of $\sim 50\%$ of an ~ 6000 s orbit mean that it is quite common to miss bursts and that the burst interval can appear to be multiples of the true value; from Figure 1 it is relatively easy to see when this occurs. Removing those points that reflect missed bursts gives a mean recurrence interval τ_{rec} of ~ 16 ks (0.14d). In Figure 1 averages of τ_{rec} are shown for several shorter intervals indicating drifts in the recurrence time from 13 ks to 18 ks. This is not unusual since jitters of up to $\sim 10\%$ in the recurrence times are found to be typical of most X-ray bursters (Lewin 1977).

The steady flux is subject to major dips approximately every 50 minutes. Sometimes less deep anomolous dips occur between major dips (Paper 1; Walter et al. 1982). In Figure 2 we show some of the OSO-8 observations with a time resolution of 82s. It can be seen that in addition to the dips there are variations in the peak non-burst flux over timescales on the order of a day. These variations are also evident in the average count rates shown in Figure 1. The errors in Figure 1 reflect the dispersion in values for the non-dip phases. While the observed count rate varies by a factor of ~ 2 , it is also associated with spectral changes (Paper 1) that give a much smaller change in the total 1-60 keV flux F_{sa} from 1.0 to 1.25×10^{-9} ergs cm^{-2} s^{-1} .

(Here and in the following the subscript "s" is used to denote the "steady" source properties and "a" the apparent quantities measured by the observer.) There is some evidence for an anti-correlation of this flux with the average interval between bursts; when the flux is low, the recurrence time is longer. It is not possible to make a meaningful test of more detailed correspondence with the available coverage, given the disruption by the dips.

Although the dips were occasionally deep, they usually did not reduce the flux to zero and bursts were observed at the edges of dips. Figure 3 shows a histogram of the phases of the 50 minute period at which the bursts occurred where phase zero is defined as the deepest dips. The distribution appears random, as would be expected if the occultations and the bursts were independent. The data are not adequate to prove that the burst source is occulted, although no bright burst peak occurred at the center of a deep dip.

B. The HEAO-1 A2 Burst

As reported in Becker et al. (1977), the bursts from MXB1916-053 have e-folding decay times as short as 5 s. For the burst observed with HEAO-1 A2 the count rates were high enough to derive useful measures of the source size and temperature on time scales short compared to this. In addition, the burst could be followed with less precision for an additional ~ 100 s. Figure 4 (upper) shows the whole HEAO-1 A2 observation by the HED (2-60 keV) and Figure 4 (lower) shows light curves in both the HED and the MED (2-20 keV) for the first 40 s of the burst. One short (30 s) low point in Figure 4 (upper) stands out as a candidate for a small absorption dip. The time 2 x 50 min. before that is a few minutes after the burst and there is no notable evidence of a dip. The deepest dip here is very shallow and short in comparison to many observed in the OSO-8 data (see Fig. 2). Thus this burst was probably not affected by a dip.

Because of the limited telemetry rate, spectral resolution was traded for temporal information: at 80 ms, the shortest time scale available, we have 2 broad band "colors". Additional bands are available every 1.28 s. We have used eight 1.28 s colors, 4 from the argon MED (Medium Energy Detector) and 4 from the xenon HED 3 (third High Energy Detector). Pulse height information was available in 64 channels every 10.24 s. During the tail of the burst, when the changes are slow compared to 10 s and when the excess over the preburst spectrum is predominantly of low energies, the MED pulse height data give the best determination of the energy spectrum. When the changes are fast compared to 10 s we can still use the 1.28 s colors to fit simple 3 parameter models. The consistency of the results was checked by comparing the spectral fits from the colors with the 10 s pulse height data. Here and in the following, in order to facilitate comparison with other burst sources, black body distributions were fitted to the burst spectra. For these fits, the column densities were about the same as required for the non-burst spectra. If we fix the column density, we can use the 80 ms data to determine a temperature and normalization. For the burst spectra in all cases we use the steady flux before the burst as background. Similar analysis procedures were used for a burst from MXB 1728-34 (Hoffman et al. 1979).

The first part of the burst is shown in Figure 5 with 80 ms resolution; the 2 colors have average energies of 5 and 11 keV, respectively. This time scale resolves the rise time to be ~ 0.3 s with a possible lag of as much as 100 ms of the high behind the low energy band. There is a suggestion of temporal structure on time scales less than 1 s during the peak. Only during the first 4 s of the burst were the fits of the 1.28 s data to a black body model significantly better than to an absorbed thin thermal-bremsstrahlung. Even for the black body model, the reduced χ^2 was ~ 3 for the 1.28 s fits at

peak intensity. When the integrated incident spectra implied by the black body fits were tested as a model for the high energy resolution 10.24s data, the χ^2 values were acceptable at a level of confidence of 5% and 1%, respectively, for the two detectors with 64 channel pulse height information. Estimates of the integrated incident spectra were generated and Figure 6 shows a comparison with the models as the burst evolved. There are slight discrepancies between model and data, similar in both detectors, which suggest that the source is indeed not exactly black. But while the blackbody model is not unique in fitting the data and the fits are not always acceptable, our data do not identify a systematic and reproducible discrepancy.

The results of the black body fits are shown in Figure 7. The quantity ϵ refers to a possible energy-independent emissivity such that the differential energy flux is $(R_a^2/d^2) \epsilon \pi B(E_a, T_a)$ where B is a Planck spectrum, d , or d_{10} in units of 10 kpc, is the distance to the source and $\pi R_a^2/d^2$ the subtended solid angle. The behavior of the temperature on timescales of 1.28s indicated in Figure 7a is typical of X-ray bursts. However, the increase in the apparent radius by more than a factor of 3 over the 10 s decay of the burst is unusual. Although initial rises and declines are common (cf. Oda 1981) the radius usually levels out during the cooling phase. In this burst it appears to gradually decline during the extended tail. Figure 7d,e, and f are based on the 80 ms data and are shown with various time resolutions. The (independent) data for the 80 ms, 1.28 s and 10.24 s time scales give results which are in reasonable agreement. The rise is associated with a temperature increase. While the uncertainties are large, there is a suggestion of temperature variations across the peak. During the first 3-4 seconds of the burst, no significant radius changes occur. The radius increase starts when

the temperature starts to decline. In this respect these changes are typical; radius changes are usually associated with changes in temperature in the black body model (which would be expected if the model is not correct as well as if the radius of the effective photosphere really changes).

C. Burst Morphology

Only two types of OSO-8 data were obtained: (1) 160 ms rates for the entire 2-60 keV band of the detector, obtained for four ~ 0.8 s intervals during each satellite spin of ~ 10 s and (2) 64 channel pulse height information accumulated over 41 s. The 160 ms data are shown for four "typical" bursts in Figure 8 (see also Becker et al. 1977 for a burst from the 1976 observation.) While coverage of any one burst is incomplete, even among these chopped light curves there appear to be a variety of types among the 1978 bursts: (a) bursts with peak fluxes of $0.7\text{--}2.0$ counts cm^{-2} s^{-1} , rise times $\lesssim 1$ sec and decays which appear smooth with time constants of ~ 5 s, (b) bursts similar to a but lasting only 2-3 s, (c) bursts with a plateau level of $\sim 0.3\text{--}0.7$ counts cm^{-2} s^{-1} lasting 7-10 s with rise times which on occasion appeared as long as 2 s, and (d) a combination of b and c, that is, a fast sharp peak and a slower decline from a plateau level. There does not appear to be a clear correspondence of these different burst types with steady flux, observed recurrence time, or phase with respect to absorption dips. The variety in the structure of the bursts has been noted in Hakucho observations of several other burst sources (Matsuoka 1981). While the behavior is reminiscent of that of the transient 1608-522 (Murakami et al. 1980), the significant correlations between type and persistent flux or type and variation in peak luminosities were not present.

The data averaged over a burst can be characterized by an average apparent kT_a that ranged from 1.5 keV (type c) to 3.4 keV (type b), consistent

with there being a correlation between intensity and temperature. However an average kT_a of 2.3 keV was obtained for one type c burst and SAS-3 results show a variety of peak temperatures for any particular peak intensity range (Cominsky 1981). If the response of the OSO-8 detector is considered, the peak intensities were between 1.7 and $4.8 \times 10^{-8} \text{ erg cm}^{-2} \text{ s}^{-1}$ (for peaks between 0.7 and $2 \text{ cts cm}^{-2} \text{ s}^{-1}$) and peak kT_a in the range 2.6 – 3.0 keV. For the same ranges the implied apparent radii of a spherical black body were $(6 \pm 2) \times d_{10} \text{ km}$, in the range of the radii seen in the HEAO-1 A2 observations.

For comparison, the burst as seen with the HEAO-1 A2 MED is plotted in Figure 8e with a time resolution of 160 ms and the same scales as in Figure 8 a-d. It seems to be intermediate between types c and d, with a sharp rise and a high temperature peak, but a relatively slow decay. The peak rate of type b bursts seen with OSO-8 and an average temperature of 3.4 keV imply an apparent radius of $4.5 \times d_{10} \text{ km}$, similar to that at the beginning of the burst seen with HEAO-1 A2 (Figure 7e). The rate for the very low temperature type c burst implies $11 \times d_{10} \text{ km}$. These results suggest a recurring correspondence of high temperature peak with "small" radius and low temperature plateau with "large" radius.

III. Derived Burst Quantities

A. Ratio of Steady to Average Burst Luminosity

The quantity $\alpha = F_{sa} \tau_r / \int F_{ba} dt$ where F_{sa} and F_{ba} are the apparent steady and burst fluxes, reflects the nuclear energy liberated in the flash from the matter which has fallen onto a neutron star. Accounting for the observed ratios of ~ 100 was an outstanding success of the Helium flash model (Joss 1978; van Paradijs et al. 1979). This ratio does depend on parameters like the neutron star mass, the type of fuel, its accretion rate and the

conditions under which it accumulates (e.g. Taam 1981a,b; Ayasli and Joss 1982), although it is not yet a clear discriminant. For MXB1916-053 the OSO-8 observations give $F_{sa} \tau_p \sim 1.7 \times 10^{-5} \text{ ergs cm}^{-2}$, approximately independent of the changes in F_{sa} because of the anticorrelation with τ_p . For the burst seen by HEAO-1 A2 $\int F_{ba} dt = 1.4 \times 10^{-7} \text{ erg cm}^{-2}$. This quantity also tended to stay constant, independent of the burst types; i.e. there is an inverse correlation of peak flux and duration. Thus during both OSO-8 observations the values of α averaged over about one day appeared to stay constant at ~ 120 .

B. Peak Luminosities

HEAO-1 A2 observed a maximum of $1.8 \times 10^{-8} \text{ ergs cm}^{-2}\text{s}^{-1}$ averaged over 160 ms. For OSO-8, peaks of $\geq 4 \times 10^{-8} \text{ ergs cm}^{-2}\text{s}^{-1}$ are indicated. The apparent luminosities, assuming a spherically symmetric source are $(2-5) \times 10^{38} d_{10}^2 \text{ ergs s}^{-1}$ implying luminosities at the surface of the neutron star of $(6 - 14) \times 10^{38} d_{10}^2 / (3 g_{00})$ where $g_{00} = 1 - 2 GM/Rc^2 = (1 + Z)^{-2}$ takes the minimum value $\sim 1/3$ for neutron star models (e.g. $M = 1.41 M_\odot$, $R = 6.5 \text{ km}$) (see Arnett and Bowers 1977). Considering that at the surface

$$L_{ED} \sim g_{00}^{-1/2} \frac{2.5}{(1+X)} 10^{38} \left(\frac{M}{M_\odot}\right) \text{ erg s}^{-1},$$

where X is the fractional abundances by mass of H, the ratio of the peak to Eddington limiting flux was

$$\frac{F}{F_{ED}} \sim (1.4-3.2) (3 g_{00})^{-1/2} (1+X) d_{10}^2 (M/M_\odot)^{-1}. \quad (1)$$

For a $1.4 M_\odot$ neutron star at 10 kpc, accreting solar abundances, this takes values 2-4, and 1-2 for accretion of He. In the spherical blackbody model (neglecting effects of magnetic field or emissivity appreciably less than

unity) the instantaneous ratio of flux to Eddington limiting flux should be, for a neutron star with $R > 3 \text{ GM}/c^2$,

$$\frac{\sigma T_a^4}{F_{\text{ED}}} \sim \frac{k T_a}{1.6}^4 (3g_{00})^{-3/2} \frac{(R/6.5 \text{ km})^2}{(M/1.4 M_\odot)} \left(\frac{1+X}{2}\right) \quad (2)$$

As Goldman (1979) pointed out, for $kT_a \sim 2\text{--}3 \text{ keV}$ this exceeds unity unless R and M are less than expected for neutron stars. We call a "standard" neutron star one with mass and radius in the range discussed by Arnett and Bowers (1977) (in particular, with an equation of state harder than that used for curve B of their Figure 11). Marshall (1982) has pointed out that under these conditions the Eddington limit is exceeded as long as $kT_a > 1.65 \text{ keV}$ for $X = 1$ and $> 1.96 \text{ keV}$ for accreting He. Conversely if a standard neutron star were black, $kT_a \sim 3 \text{ keV}$ would imply $\gtrsim 9$ times the Eddington limiting flux for solar abundances. We note however that this interpretation would imply for the HEAO-1 A2 burst $d_{10} = 2.3 (3g_{00})^{-1/2} (R/6.5 \text{ km})$, which is always greater than 2 for the allowed M and R . Thus for this source emissivity or asymmetry is important, if the source is not to be on the other side of our galaxy.

C. Radius of a Spherical Black Body

The apparent "radii", or more generally, $\epsilon^{1/2} R_a/d_{10}$, derived from the data ranged from 4–15 km. Then for a sphere with $R > 3 \text{ GM}/c^2$,

$$R = (3 g_{00})^{1/2} (2.3 - 8.6) \frac{d_{10}}{\epsilon^{1/2}} \text{ km} \quad (3)$$

The smaller value refers to the first 3s of the burst, the large value to the average high values 20–40 s after the onset.

D. Accretion Rate

The steady flux arises from mass accretion at a rate \dot{M} at the neutron star surface which appears from afar to be $\dot{M}_a = g_{00}^{1/2} \dot{M}$. The rate of energy released is

$$L = \dot{M} c^2 [g_{00}^{-1/2} - 1] \quad (4)$$

with $L_x = \zeta L$ appearing in the X-ray band. Here

$$L_x = g_{00}^{-1} f^{-1} F_{sa} 4\pi d^2, \quad (5)$$

where the correction factor f represents asymmetry in the emission of effects of limb darkening or obscuration (cf. Milgrom 1978) which might be expected for the high inclination implied by the absorption dips. Thus the observed steady flux implies

$$\dot{M}_a = f^{-1} \zeta^{-1} \frac{1 - 1/3^{1/2}}{1 - g_{00}^{1/2}} 4.7 \times 10^{-10} \frac{F_{sa}}{10^{-9}} d_{10}^2 M_\odot \text{ yr}^{-1}. \quad (6)$$

If the steady emission is not beamed and $f < 1$

$$\dot{M}_a > 4.7 \times 10^{-10} d_{10}^2 M_\odot \text{ yr}^{-1}. \quad (7)$$

IV. EVOLUTIONARY CONSIDERATIONS

In the following we assume that the mass losing star approximately fills its Roche lobe. The combination of the Roche lobe relation for mass ratios less than 0.8 and Kepler's third law yield the well known relation $P \sqrt{\rho} = 3.78 \times 10^4$ (Faulkner, Flannery and Warner 1972), where P and ρ represent the

orbital period and the mean density of the mass losing component respectively. For a 50 minute orbital period the secondary's mean density is 159 gm cm^{-3} . In such a tight binary system a lower limit to the mass exchange rate can be estimated from the loss of angular momentum via gravitational radiation (GR) (Faulkner 1971; Paczynski 1967). If the evolution driven by GR (or evolution driven by some other mechanism) is rapid compared to the thermal time scale of the mass losing star, thermal disequilibrium effects will be important (Paczynski 1981). It is convenient to separate the discussion into the cases where such thermal effects are not (case I) or are (case II) important. The results are summarized in Table 1.

A. Case (I) -- Thermal Equilibrium

If thermal disequilibrium effects are not important, one can adopt equilibrium mass-radius relations. As stated in Paper I, possible solutions include (1) a $1.11 M_{\odot}$ He main sequence star (based upon models calculated by Paczynski 1971), (2) a $0.044 M_{\odot}$ "hydrogen" ($X = 0.75$) white dwarf and (3) a $0.009 M_{\odot}$ He white dwarf (the latter two solutions based on the models calculated by Vila 1971). No self consistent solution for a hydrogen main sequence star was given in Paper I, since the best estimates of the mass radius relation for the lower main sequence imply a mass ($0.076 M_{\odot}$) below the minimum for hydrogen burning ($0.085 M_{\odot}$ according to Graboske and Grossman 1971). The difference is small however and subtleties in the treatment of the equation of state might affect the calculated endpoint of the main sequence or the mass radius relation, so that a hydrogen burning companion may still be possible. Recently, D'Antona and Mazzitelli (1982) have constructed low mass models assuming constant mass loss rates.

For $\dot{M} \leq 10^{-12} M_{\odot} \text{ yr}^{-1}$, (corresponding to models which are in thermal equilibrium) their models give the inferred mean density at ~ 0.093 and 0.10

M_\odot for $Z = 0.02$ and 0.001 , respectively (where Z is the metal abundance by mass).

By generalizing the expression for mass transfer rates induced by gravitational radiation losses, assuming conservative mass transfer (cf. Faulkner 1971) one obtains, for a $1.4 M_\odot$ neutron star, mass transfer rates of 6×10^{-8} , 7×10^{-11} , and $3 \times 10^{-12} M_\odot \text{ yr}^{-1}$ for solutions (1), (2) and (3), respectively. For hydrogen burning main sequence mass-radius relation quoted by Whyte and Eggleton (1981) (extrapolated below $0.085 M_\odot$) we find a mass exchange rate of $1 \times 10^{-10} M_\odot \text{ yr}^{-1}$. If instead we take $R \sim M$, (used by Li et al. 1980), the mass exchange rate is 80% higher. The models by D'Antona and Mazzitelli for constant, low mass loss rates imply $\sim 2 \times 10^{-10} M_\odot \text{ yr}^{-1}$. For the solutions with secondary masses $\lesssim 0.1 M_\odot$, the mass transfer rate is proportional to $M_x^{2/3}$, where M_x is the neutron star mass, so that a higher M_x could increase the rate only about 50%.

B. Case II -- Thermal Disequilibrium

Whenever the mass transfer proceeds on a time scale which is short compared to the thermal time scale of the mass losing component, the thermal history of the latter will affect the stellar radius. In fact, a sizable departure from thermal equilibrium mass radius relations is expected. RJW have recently investigated the evolution of binary systems composed of main sequence stars and compact objects with gravitational radiation losses included. As pointed out in RJW, the effect of thermal disequilibrium becomes pronounced as the system approaches its minimum orbital period. A minimum period is expected due to the transition in stellar structure from a hydrogen burning star to a degenerate one. If we adopt their case 6 which corresponds to a hydrogen depleted composition with $X = 0.2$ and interpolate in their Figure 8, we obtain a mass of about $0.04 M_\odot$ for the mass losing star. The

corresponding mass transfer rate near the minimum period of 46.5 minutes is approximately $4 \times 10^{-11} M_{\odot} \text{ yr}^{-1}$.

Departure from thermal equilibrium can also be important for secondaries composed of a helium core and a hydrogen rich envelope. Such composite models were suggested by Faulkner, Flannery, and Warner (1972) as possible progenitors to HZ 29 = AM CVn. For such evolved secondaries, the stellar envelope would contract once its mass reached a critical minimum value (cf. Refsdal and Weigert 1971). Consequently, mass transfer would cease as the star no longer would fill its Roche lobe. However, since the rate of stellar contraction decreases as the secondary evolves to the white dwarf stage, the loss of angular momentum by gravitational radiation would eventually reduce the size of the Roche lobe until mass transfer is reinitiated. In such an evolutionary scheme a mass transferring system at the 50 min. orbital period is a distinct possibility. We have computed such an evolutionary sequence for low mass composite secondaries ($M = 0.11$ and $0.15 M_{\odot}$) in order to test this conjecture.

The initial models are characterized by a Population I composition ($X = 0.70$, $Y = 0.28$, and $Z = 0.02$) and were constructed and evolved utilizing the stellar structure program described in Eggleton (1971,1972). The assumptions and constitutive relations are described in Taam (1983). The two model stars were evolved at constant mass to the envelope contraction phase and then placed in a binary. The period and total binary mass corresponded to 50 min and $1.51 M_{\odot}$ and 58 min. and $1.55 M_{\odot}$ for sequences 1 and 2 respectively. The results for both sequences are summarized in Table 1. We find that mass transfer rates as high as $\sim 2 \times 10^{-10} M_{\odot} \text{ yr}^{-1}$ can be achieved at an orbital period of 48 min for sequence 1, while for sequence 2 the mass transfer rate is lower ($0.4 \times 10^{-10} M_{\odot} \text{ yr}^{-1}$). The mass transfer rates for each sequence are

plotted as a function of orbital period in Figure 9. Secondaries as massive as $0.15 M_{\odot}$ contract rapidly at these periods implying low mass transfer rates. A third sequence (characterized by a secondary of $0.11 M_{\odot}$ and an initial period of 71 min) was calculated to determine the effect of even lower mass secondaries at 50 min. It is found that the mass transfer promoted by gravitational radiation is slower than for sequence 1 because the angular momentum losses are less efficient for smaller mass stars at a given orbital period ($M \sim 0.052 M_{\odot}$ at a 48 min orbit).

V. COMPARISON WITH THE OBSERVATIONS

Assuming GR to be the dominant driver of mass exchange, one can constrain the distance for each of the models discussed in the previous section. Since the inferred mass transfer rate is $> 4.7 \times 10^{-10} d_{10}^2 M_{\odot} \text{ yr}^{-1}$ (see eq. 7), the source would have to be closer than 5 kpc for the solutions with $\dot{M}_a \lesssim 10^{-10} M_{\odot} \text{ yr}^{-1}$. For the He degenerate solution the limiting distance would be ~ 1 kpc. For the H depleted ($X = 0.2$) solution in which thermal disequilibrium is taken into account in the evolution the distance is ~ 3 kpc. For the composite model GR would saturate the mass exchange at 6.0–6.5 kpc.

The He main sequence solution was ruled out in paper I and by Walter et al. (1982) on the basis of the optical appearance of the source. The bursts provide another argument against it, if we assume the type I bursts are thermonuclear runaways in freshly accreted layers on a neutron star (Joss 1978; Taam and Picklum 1979). The solution implies gravitational radiation driving the mass exchange at such a high rate (in excess of the rate for which the steady luminosity equals the Eddington luminosity) that the luminosity from the nuclear outburst would not be sufficient to dominate that from accretion. The He degenerate secondary solution (see above) is also inconsistent with the burst data. In particular, the expected burst

recurrence times would be more than an order of magnitude longer than those observed. Thus all solutions involving a He secondary are very unlikely.

Thermonuclear flash theory (Joss 1978; Taam 1981a,b, 1982; Ayasli and Joss 1982) predicts that the peak burst luminosity does not exceed the Eddington limit. Based upon equation (1) the peak luminosities of most bursts observed from the source would be equal to the Eddington limit at ~ 6 kpc. Thus, the composite model provides a self-consistent scenario if the bursts peak at about the Eddington limit. However, there is evidence that points to burst luminosities exceeding the Eddington limit by factors of 2-10 even if black body emission is not assumed (Inoue et al. 1980; van Paradijs 1981). Thus, comparison with other bursters would favor a distance near 10 kpc if the galactic center is ~ 9 kpc away and not as close as 7 kpc (cf. Frenk and White 1982; Glass and Feast 1982). The distribution of known burst sources about the galactic center is uncertain, but as Inoue et al. (1980) discussed, the group is unlikely to be clustered far from the galactic center. Thus the composite model solution is only marginally consistent with both GR and results on other bursters. Furthermore we must bear in mind that to get this consistency we are forced to use the lower limit on the mass transfer rate.

If the assumption is made of spherical black bodies, comparison of the luminosities of the bursters is nearly the same as comparison of the radii, since the temperatures of the black body fits are typical. The values of $\epsilon^{1/2} R_c \sim (4-15) d_{10} \text{ km}$ observed for bursts from MXB1916-053 are near the range 5-12 km observed for other bursters (Inoue et al. 1980; van Paradijs 1978) and would still overlap this range if $d_{10} = 0.6$.

Ayasli and Joss (1982) and Taam (1981a,b, 1982) find that for short recurrence times of less than 5 hours the hydrogen rich layers participate in the flash (see also Fujimoto, Hanawa and Miyayai 1981) and the mass accretion

rates should exceed $\sim 5 \times 10^{-10} M_{\odot} \text{ yr}^{-1}$, (although effects due to the evolving thermal state and compositional history of the neutron star envelope could reduce this rate somewhat). This is in agreement with the observed steady flux if the source is near 10 kpc. At this distance the bursts, then, are more typical in peak luminosity and inferred radii to other burst sources. In addition nuclear flashes of this type (H-He) are consistent with $\alpha \sim 120$ found for this source.

VI. DISCUSSION

If the burst emission is spherically symmetric from the entire surface, flash theory (at least in the limit cycle approximation) implies a mass transfer rate higher than GR can drive from any of the types of secondary considered in §IV, except possibly the composite model (with $M \sim 0.1 M_{\odot}$). A spherically symmetric steady source is then at such a distance (10 kpc) that the burst luminosities are typical.

For 4U1626-67, Joss, Avni and Rappaport (1978) and Li et al. (1980) concluded that GR was marginally sufficient to drive the mass exchange for a $0.1 M_{\odot}$ hydrogen burning secondary because the $10^{-9} M_{\odot} \text{ yr}^{-1}$ estimated from the spin up rate was very uncertain. For MXB1916-053/4U1915-05 the bursts constrain the exchange rate. In both cases the discrepancy with GR is least for a secondary at the end of the main sequence and is minimally a factor of ~ 2 . This discrepancy is not so much greater than the uncertainties in the arguments as to be unquestionable but a second source now shows the same discrepancy on the basis of quite different arguments.

Several mechanisms have been appealed to for driving higher rates of mass transfer than seems possible with GR alone. Nuclear evolution (Faulkner 1974; Joss, Avni and Rappaport 1978; RJW) may be a likely possibility for more massive systems with periods longer than $\sim 4^{\text{h}}$. For lower mass systems the

mechanisms of (1) "magnetic braking" and (2) transport of angular momentum out of the system with ejection of some material in the mass exchange process may be important.

Coronal magnetic field structures may force matter to corotate to large distances, so that if it then escapes, it carries off substantial angular momentum. Even if matter does not escape, the interaction of the fields and corona with surrounding material may exert a torque. The angular momentum that could be carried away by modest mass loss ($10^{-12} M_{\odot} \text{ y}^{-1}$) has long been recognized to be significant and can influence binary evolution (Mochnacki 1981 and references therein). Verbunt and Zwaan (1981) estimated that if the empirical braking law of single stars can be carried over to the close binary situation, this should only dominate over GR for secondary masses above $0.3 M_{\odot}$. The limit can be reduced to about $0.1 M_{\odot}$ (Taam 1983) when the effects due to thermal disequilibrium and the change in the moment of inertia of the mass losing star are included. Rappaport, Verbunt and Joss (1983) found that with different braking laws, magnetic braking would dominate for lower masses, but the minimum periods of those models were too long. While it seems probable that these calculations cannot adequately represent the binary situation, the effect seems likely to be important for low mass non-degenerate and possibly magnetic degenerate companions.

A large amount of angular momentum must be removed from the exchanged material before it accrete onto the neutron star and it seems plausible that some, if not a large fraction, is ejected from the system. Paczynski (1967) considered an exchange of angular momentum with an outer ring of the disk. The angular momentum may return to the orbit (Papaloizou and Pringle 1977; Weber 1979), but perhaps this could be prevented by effects not yet fully considered. Self-excited winds as a way of ejecting angular momentum was

noted by many authors and indeed Begelman, McKee and Shields (1983) have found that a substantial wind is expected. The effect does not turn out to be substantial on the evolution of binaries with non-degenerate companions (Whyte and Eggleton 1980; Kieboom and Verbunt 1981; RJW), and RJW showed this should be true for any model in which the mass loss is proportional to the mass exchanged. However, as we have shown, for this source a rather modest factor of 2 may be all that is needed. This mechanism might be even more important for a degenerate mass losing star. Kieboom and Verbunt (1981) noted that for the case of standard abundances, if a small amount of matter carried off the angular momentum, an order of magnitude effect could result; the mass exchange for a $0.05 M_{\odot}$ degenerate companion was as high as $10^{-9} M_{\odot} \text{ yr}^{-1}$ for $\sim 10^6 \text{ yr}$.

VII. SUMMARY

We have used the burst properties of the 50 min binary MXB1916-035 to estimate the mass transfer rate between the binary components and hence investigate the consistency of the GR evolutionary scenarios developed to date. Both degenerate and non-degenerate helium secondaries are incompatible with the burst properties and can be ruled out. If it is assumed that the peak burst flux is at least at the Eddington limit then a hydrogen degenerate companion will give a mass transfer rate at least a factor of 3 below that implied by the steady flux. On the other hand, the composite, inhomogeneous model is marginally consistent with the GR driven mass transfer rate. Current flash theory prefers a rate larger by about a factor of 2 as does comparison of its burst properties to other sources. In that case there may be another, dominant mechanism for losing angular momentum from the system. Recent work implies that if the angular momentum extracted from the accretion disk is lost from the system rather than fed back into the orbit, the transfer driven by GR could be sufficiently enhanced. Magnetic braking is another possible

influence, although probably more important for more massive secondaries.

ACKNOWLEDGMENTS

We are grateful for the UCSC 1981 Summer Workshop on "Cataclysmic Variables and Related Systems", where this work was conceived. JHS thanks the Institute of Astronomy, Cambridge, England, where it was completed under a Royal Society Guest Research Fellowship. RET is pleased to acknowledge support by the NSF grant AST-8109826. We thank Peter Eggleton, Richard Kelley, Walter Lewin, Frank Verbunt, and Charles Whyte for helpful discussions.

TABLE 1
POSSIBLE SOLUTIONS FOR THE SECONDARY

TYPE	$M(M_{\odot})$	$R(R_{\odot})$	$\dot{M}_{GR}(M_{\odot} \text{ yr}^{-1})$	REFERENCE
<u>Equilibrium</u>				
H burning	0.076	0.088	9.78×10^{-11}	a
$Z = 0.02$	0.094	0.094	1.78×10^{-10}	b
	0.098	0.096	1.70×10^{-10}	c
$Z = 0.001$	0.103	0.097	2.03×10^{-10}	c
He burning	1.111	0.215	6.14×10^{-8}	d
H degenerate ($X = .75$)	0.044	0.073	6.96×10^{-11}	e
He degenerate	0.009	0.043	2.82×10^{-12}	e
<u>Non-equilibrium</u>				
H burning ($X = .2$)	~ 0.04	0.07	$\sim 4.0 \times 10^{-11}$	f
Composite	0.11	0.10	1.8×10^{-10}	g
	0.15	0.11	4.0×10^{-11}	
OBSERVED	----	----	$> 4.7 \times 10^{-10} d_{10}^2$	

^a Whyte and Eggleton (198C)

^b Li et al. (1980)

^c D'Antona and Mazzitelli (1982)

^d Paczynski (1971b)

^e Vila (1971)

^f Rappaport, Joss and Webbink (1982)

^g this paper

REFERENCES

- Arnett, W.D., and Bowers, R.L., 1977, *Ap. J. Suppl.* 33, 415.
- Ayasli, S., and Joss, P.C., 1982, *Ap. J.* 256, 637.
- Becker, R.H., Smith, B.W., Swank, J.H., Boldt, E.A., Hoit, S.S., Pravdo, S.H.,
and Serlemitsos, P.J., 1977, *Ap. J. (Letters)* 216, L101.
- Begelman, M.C., McKee, C.F. and Shields, G.A., 1982, *Ap. J.* 271, 70.
- Cominsky, L., 1981, Ph.D. thesis, Massachusetts Institute of Technology.
- Cowley, A.P., and Crampton, D., 1975, *Ap. J. (Letters)* 201, L65.
- Cowley, A.P., Crampton, D., and Hutchings, J.B., 1979, *Ap. J.* 231, 539.
- D'Antona, F., and Mazzitelli, I., 1982, *Astron. Ap.* 113, 303.
- Eggleton, P., 1971, *MNRAS* 151, 351.
- Eggleton, P., 1972, *MNRAS* 156, 361.
- Faulkner, J., 1971, *Ap. J. (Letters)* 170, L99.
- Faulkner, J., 1974, in *IAU Symp. No. 66, "Late States of Stellar Evolution"*,
ed. R.J. Taylor (Dordrecht: Reidel), p. 155.
- Faulkner, J., Flannery, B.P., and Warner, B., 1972, *Ap. J.* 175, L79.
- Frenk, C.S., and White, S.D.M. 1982, *MNRAS* 198, 173.
- Fujimoto, M.Y., Hanawa, T., and Miyaji, 1981, *Ap. J.* 247, 267.
- Glass, I.S., and Feast, M.W., 1982, *MNRAS* 198, 199.
- Goldman, I., 1979, *Astr. Ap.* 78, L15.
- Graboske, H.C., and Grossman, A., 1971, *Astrophys. J.* 170, 363.
- Hoffman, J.A. et al. 1979, *Ap. J. (Letters)* 233, L51.
- Inoue, M., et al., 1981, *Ap. J.* 250, L71.
- Joss, P.C., 1978, *Ap. J. (Letters)* 225, L123.
- Joss, P.C., Avni, Y., and Rappaport, S., 1978, *Ap. J.* 221, 645.
- Joss, P.C., and Rappaport, S., 1979, *Astr. Ap.* 71, 217.
- Kieboom, K.H., and Verbunt, F., 1981, *Astr. Ap.* 95, L11.

- Lewin, W.H.G., 1977, Ann. N.Y. Acad. Sci. 302, 210.
- Lewin, W.H.G., 1982a, Proceedings of the Symposium on Neutron Stars, MIT preprint, CSR-HEA-82-3.
- Lewin, W.H.G., 1982b, in Accreting Neutron Stars, ed. W. Brinkman and J. Trumper, p. 77, Max-Planck-Institut ISSN 0340-8922, Garching Bei Munchen, W. Germany.
- Lewin, W.H.G., Hoffman, J.A., and Doty, J., 1977, IAU Circ. No. 3087.
- Li, F.K., Joss, P.C., McClintock, J.E., Rappaport, S., and Wright, E.L., 1980, Ap. J. 240, 628.
- Marshall, H.L., 1982, Ap. J. 260, 815.
- Marshall, H.L., and Millet, N., 1981, Nature 293, 379.
- Mason, K.O., Middleditch, J., Nelson, J.E., White, N.E., Seitzer, P., Tuohy, I.R., and Hunt, L.K., 1980, Ap. J. (Letters) 242, L109.
- Matsuoka, M., 1981, Symposium on Space Astrophysics, p. 88, Univ. of Tokyo, Japan.
- McClintock, J.E., and Petro, L.D., 1981, IAU Circ. No. 3615.
- Middleditch, J., Mason, K.O., Nelson, J.E., White, N.E., 1981, Ap. J. 244, 1001.
- Milgrom, M., 1978, Astr. Ap. 67, L25.
- Mochancki, S.W. 1981, Ap. J. 245, 650.
- Murakami, T. et al., 1980, Ap. J. (Letters) 240, L143.
- Oda, M., 1981, Plasma Astrophysics, Proc. of a Course and Workshop held in Varenna (Como), Italy, ed. T.D. Guyenne and G. Levy, ESA SP-161.
- Paczynski, B., 1967, Acta Astr. 17, 287.
- Paczynski, B., 1971, Acta Astr. 21, 1.
- Paczynski, B., 1981, Acta Astr. 31, 1.
- Paczynski, B., and Sienkiewicz, R., 1981, Ap. J. 248, L27.

- Papaloizou, J. and Pringle, J.E., 1977, M.N.R.A.S. 181, 441.
- Pedersen, H., van Paradijs, J., and Lewin, W.G.H. 1981, Nature 294, 725.
- Rappaport, S., Joss, P.C., and Webbink, R.F., 1982, Ap. J., in press.
- Rappaport, S., Verbunt, F., and Joss, P.C. 1983, Ap. J., in press.
- Refsdal, S., and Weigert, A., 1971, Ast. Ap. 13, 367.
- Swank, J.H., Eardley, D.M., and Serlemitsos, P.J., 1979, unpublished preprint.
- Taam, R.E. 1981a, Ap. J. 247, 257.
- Taam, R.E. 1981b, Ap. Space Sci. 77, 257.
- Taam, R.E. 1982, Ap. J. 258, 761.
- Taam, R.E. 1983, Ap. J. 268, 361.
- Taam, R.E., and Picklum, R.E. 1979, Ap. J. 233, 327.
- Thorstensen, J., Charles, P., Bowyer, S., Briel, U.G., Doxsey, R.E., Griffiths, R.E., and Schwartz, D.A., 1979, Ap. J. (Letters) 233, L57.
- van Paradijs, J., 1978, Nature 274, 650.
- van Paradijs, J., Joss, P.C., Cominsky, L., and Lewin, W.H.G., 1979, Nature 280, 375.
- van Paradijs, J., Rybicki, G., and Lamb, D.Q., 1979, Bull. A.A.S. 11, 788.
- van Paradijs, J., 1981, Astr. Ap. 101, 74.
- van Paradijs, J., 1982, Astr. Ap. 107, 51.
- Verbunt, F., and Zwaan, C., 1981, Astr. Ap. 100, L7.
- Vila, S.C., 1971, Ap. J. 168, 217.
- Walter, F.M., Bowyer, S., Mason, K.O., Clark, J.T., Henry, J.P., Halpern, T., and Grindlay, J.E., 1982, Ap. J. (Letters) 253, L67.
- Watson, M., 1976, MNRAS 176, 16p.
- Weber, S.V., 1979, Ap. J. 229, 327.
- White, N.E., and Swank, J.H., 1982, Ap. J. (Letters) 253, L61 (Paper 1)
- Whyte, C.A., and Eggleton, P., 1980, M.N.R.A.S. 190, 801.

FIGURE CAPTIONS

Figure 1 (upper) - Time since the last burst observed during the OSO-8 observations (\bullet). The lines are averages of intervals between successive bursts. See text for definition of burst types a-d. (bottom) - Average non-dip count rate as a function of time.

Figure 2 - Counts $\text{cm}^{-2}\text{s}^{-1}$ averaged over 82s for 2 intervals ~ 1 d long of OSO-8 observations from 1978 March. Typically, every other dip was obscured by earth occultation. The average non-dip count rates were variable by almost a factor of 2. Altogether ~ 50 dips were observed.

Figure 3 - Histogram of number of bursts falling in phase intervals of 0.1 relative to the phase of dip center for 1976 (hatched) and for 1978 (open).

Figure 4 (upper) - Light curve of 4U1916-05 with the HEAO-1 A2 HED, similar to the detector used in the OSO-8 observations but with 2.9 times the area. Arrows point out a dip and the times when the same phase of a 50 min period was covered. (lower) - The HED and MED burst light curves with 1.28 s resolution for the first 40s of the burst.

Figure 5 - The first 8 s of a burst are shown with 80 ms resolution in the MED (argon) detector (upper) for which the average energy is 5 keV and the second layer of the HED3 (xenon) detector (lower) with average energy of 11 keV.

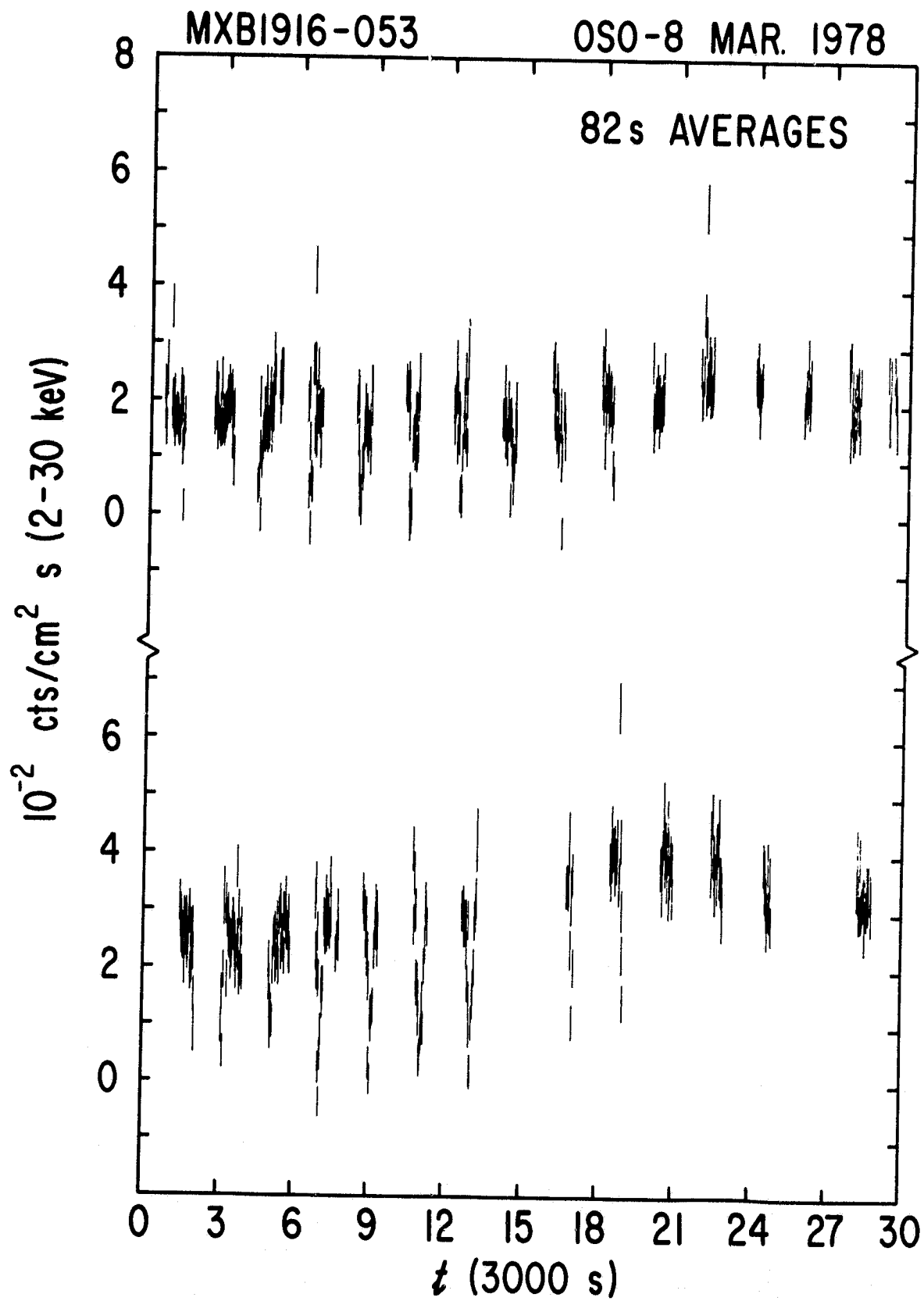
Figure 6 - Average incident spectra for three intervals of the burst seen by HEAO-1 A2.

Figure 7 - The spectral parameters derived for the HEAO-1 A2 burst. (a) kT_a obtained from 1.28 s color fits (solid crosses) and 10.24 s pulse height data (dashed crosses) (b) $\epsilon^{1/2} R_a/d_{10}$ for the same fits (c) flux (1-60 keV) for the unabsorbed black body spectral model; the solid line is the integrated energy per unit area received from the burst, for which the scale is 10^{-7} ergs cm^{-2} . (d) kT_a for the beginning of the burst from the 80 ms data: 320 ms averages (dashed crosses) and shorter averages (solid crosses) along with the 1.28 s results (—). (e) $\epsilon^{1/2} R_a/d_{10}$ for the same as (d). (f) Flux for the same as (d).

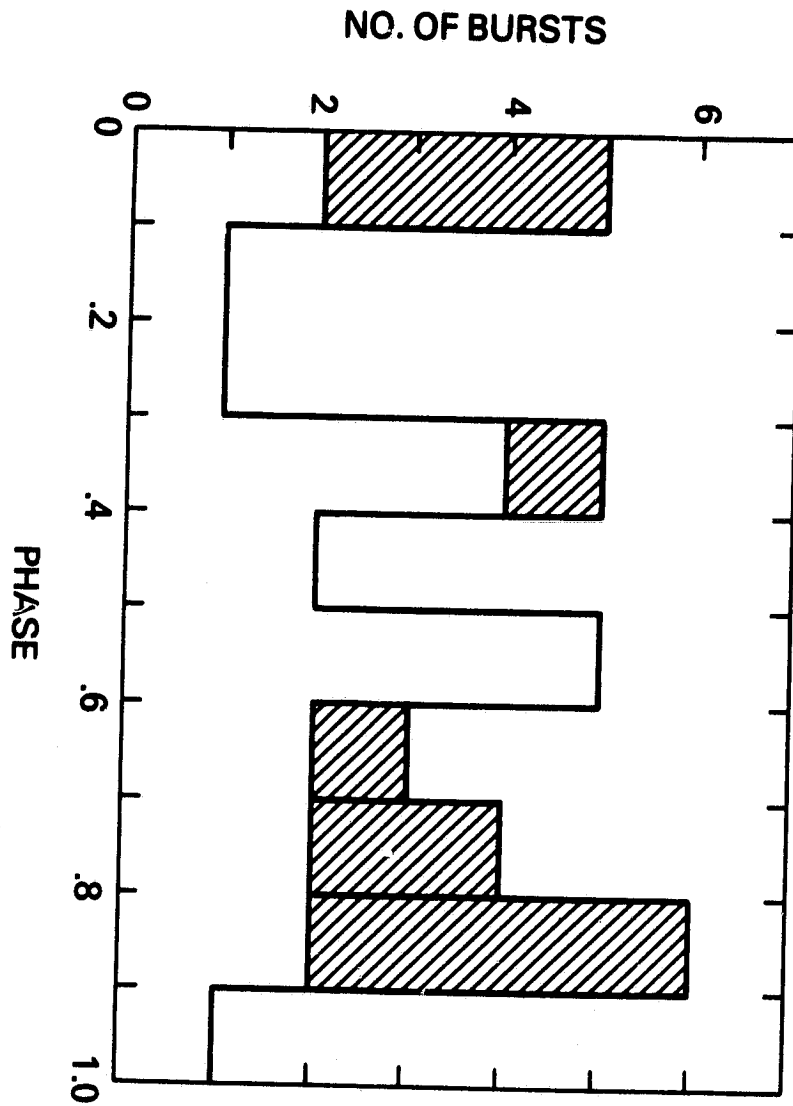
Figure 8 - Light curves of 50 s of 4 OSO-8 bursts and the 1 HEAO-1 A2 burst with 160 ms time resolution. (a), (b), (c) and (d) refer to the 4 types discussed in the text. The HEAO-1 A2 light curve is from the MED.

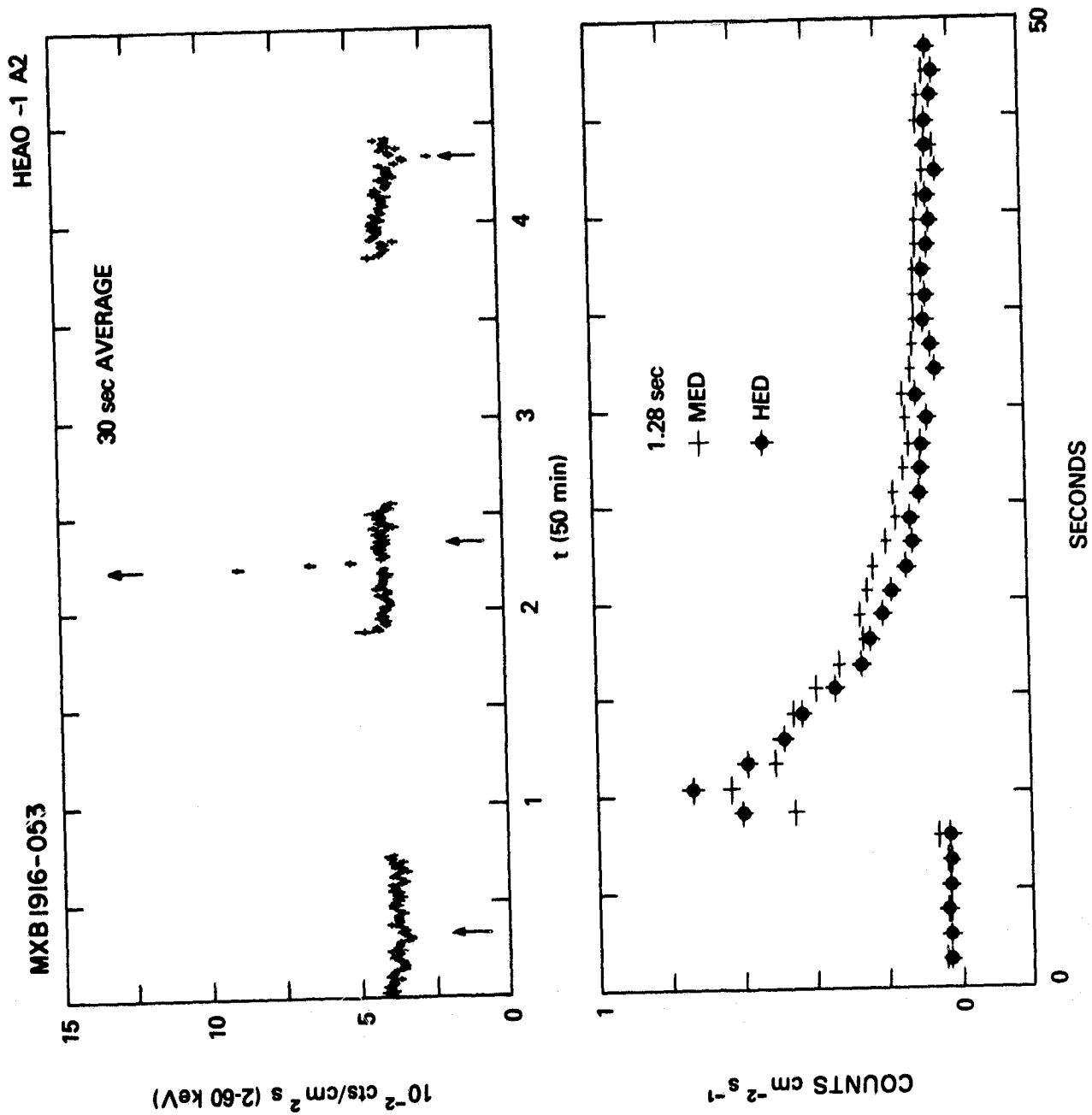
Figure 9 - Mass exchange rate driven by GR as a function of the binary period for three sequences. The secondary mass (in M_\odot) is indicated at selected times during the evolution.

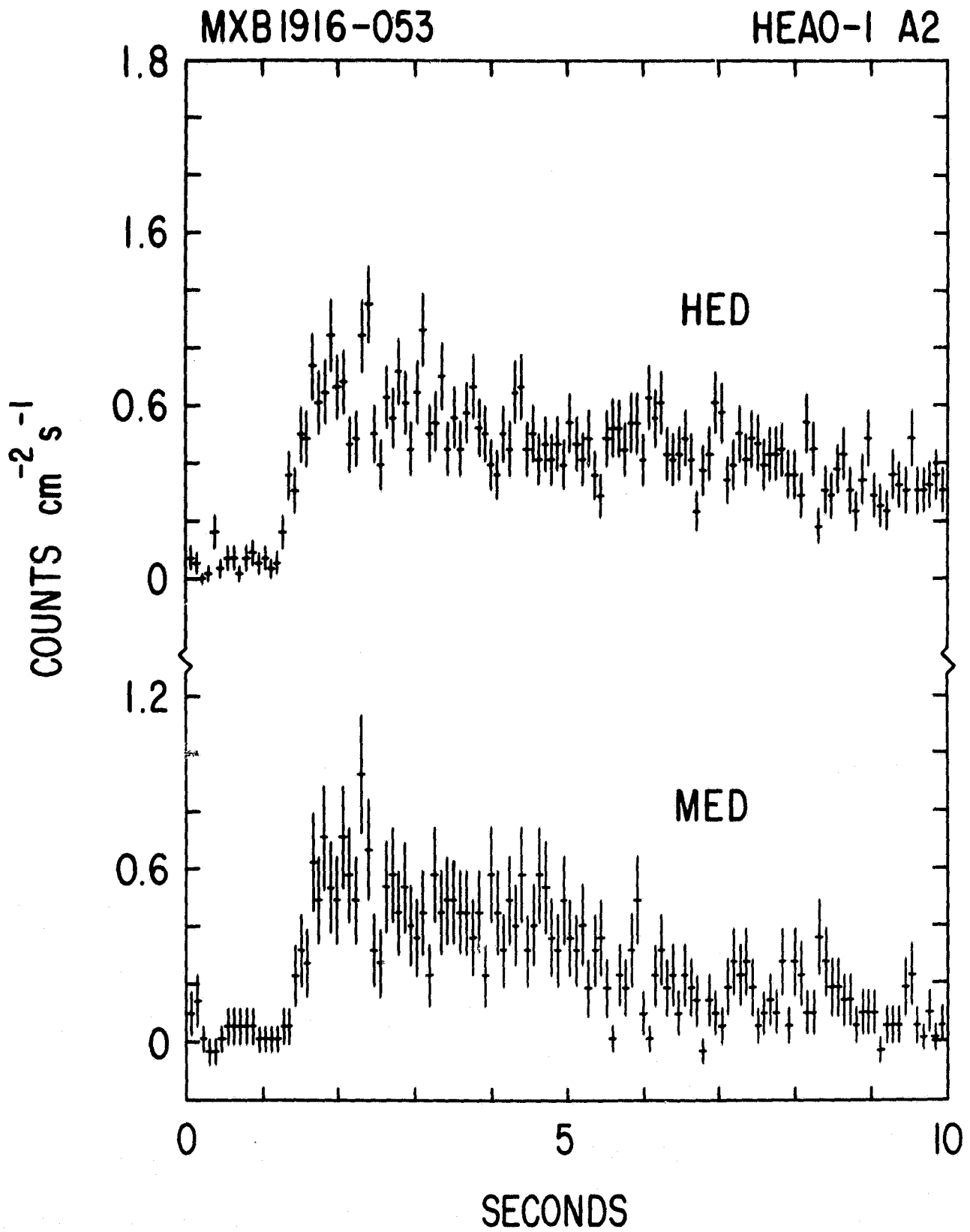
050-8



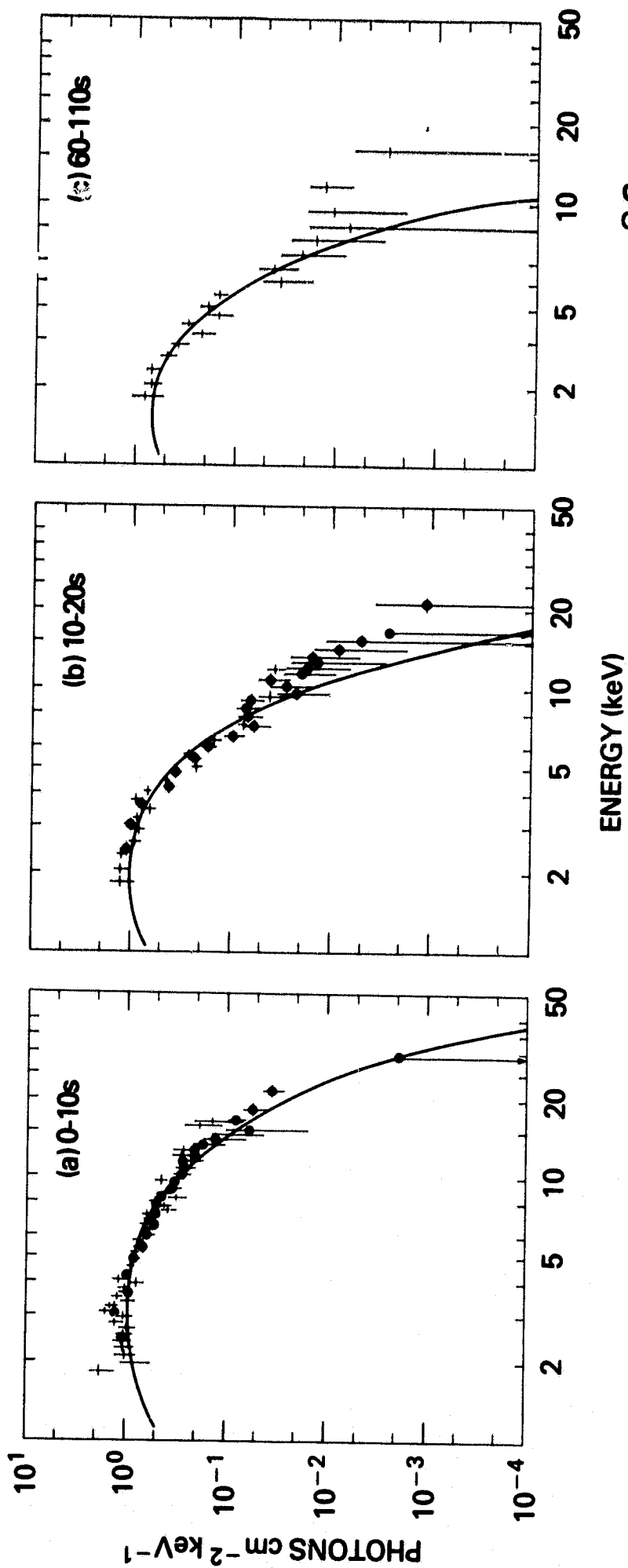
ORIGINAL PAGE IS
OF POOR QUALITY



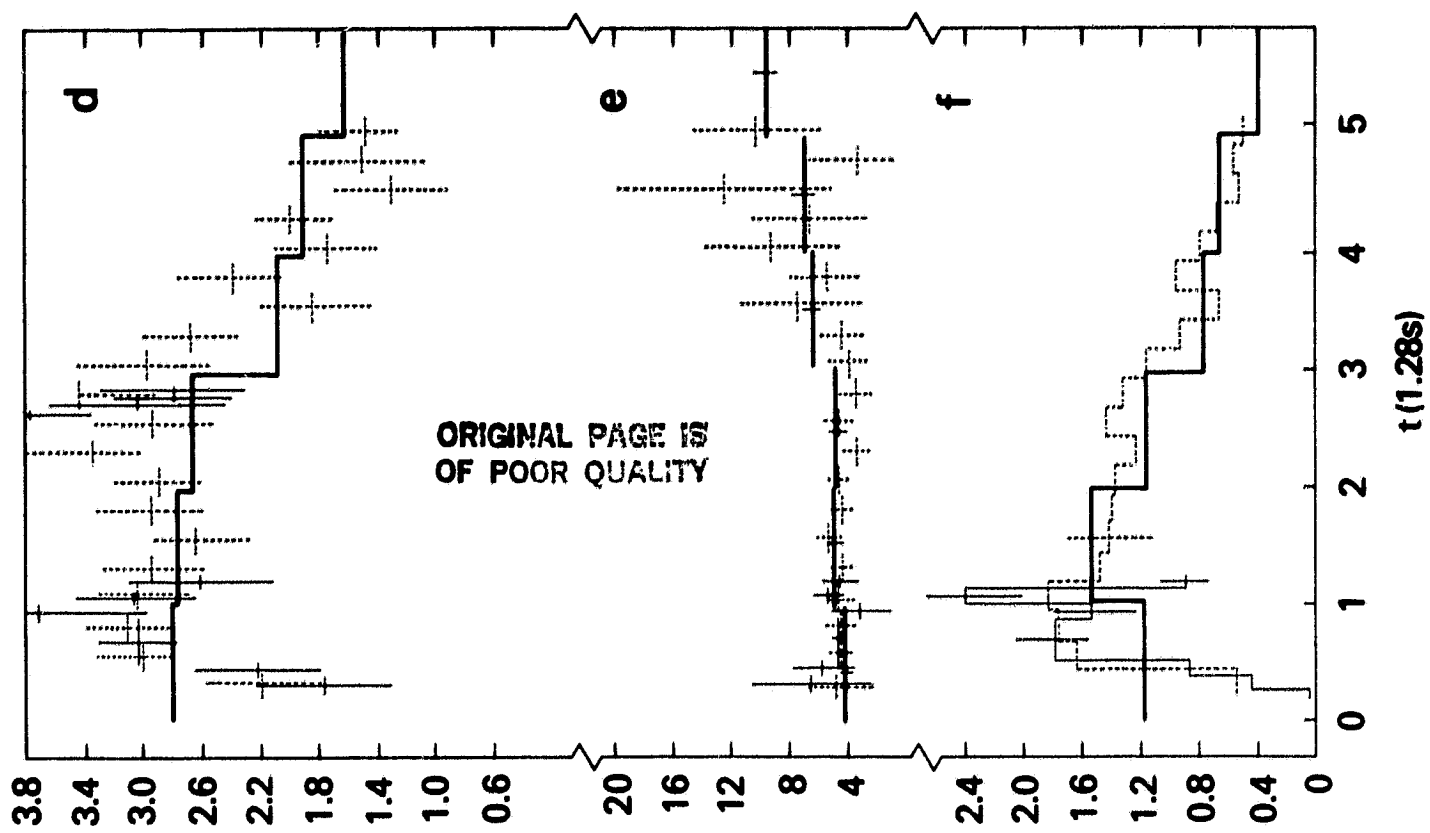
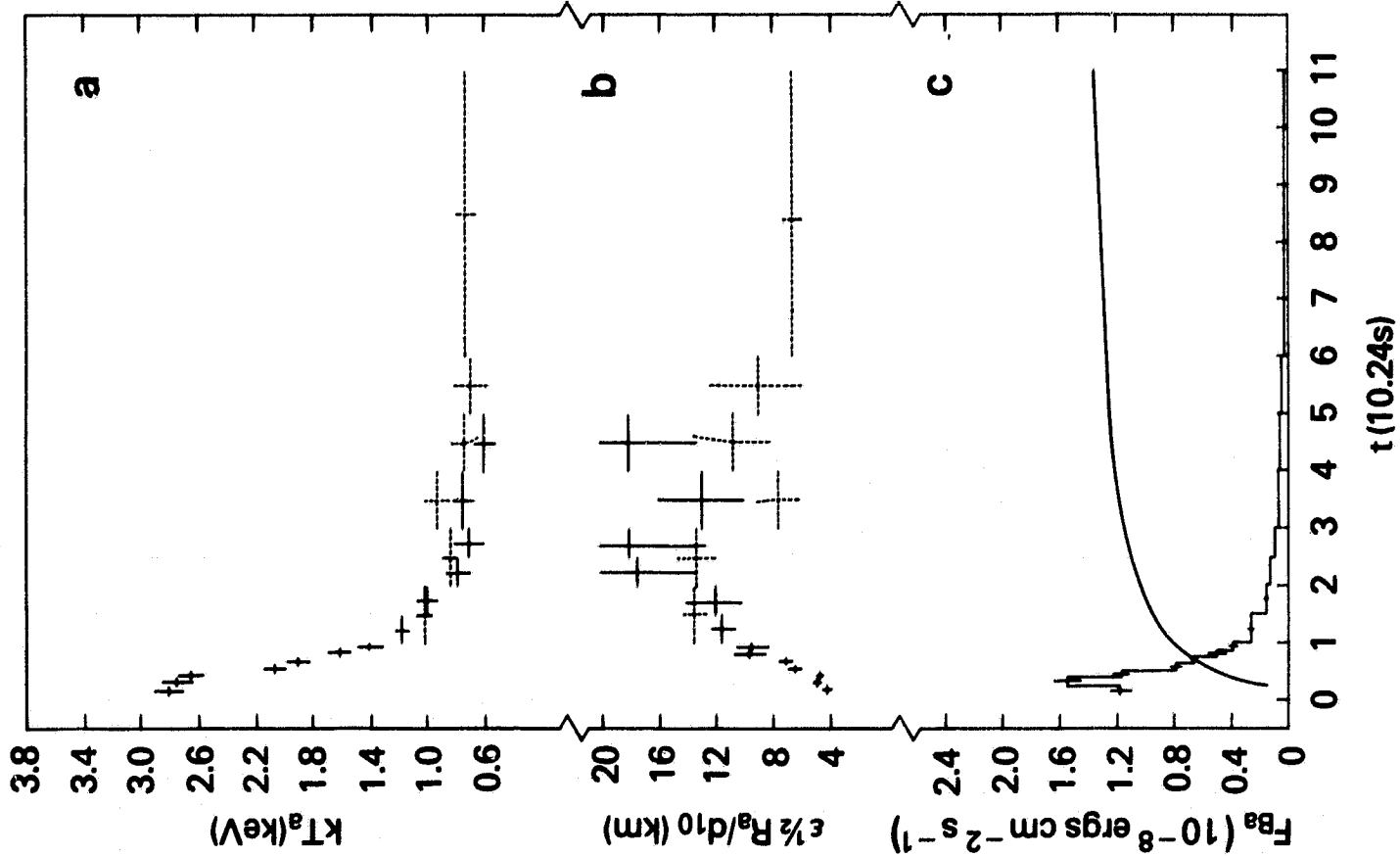




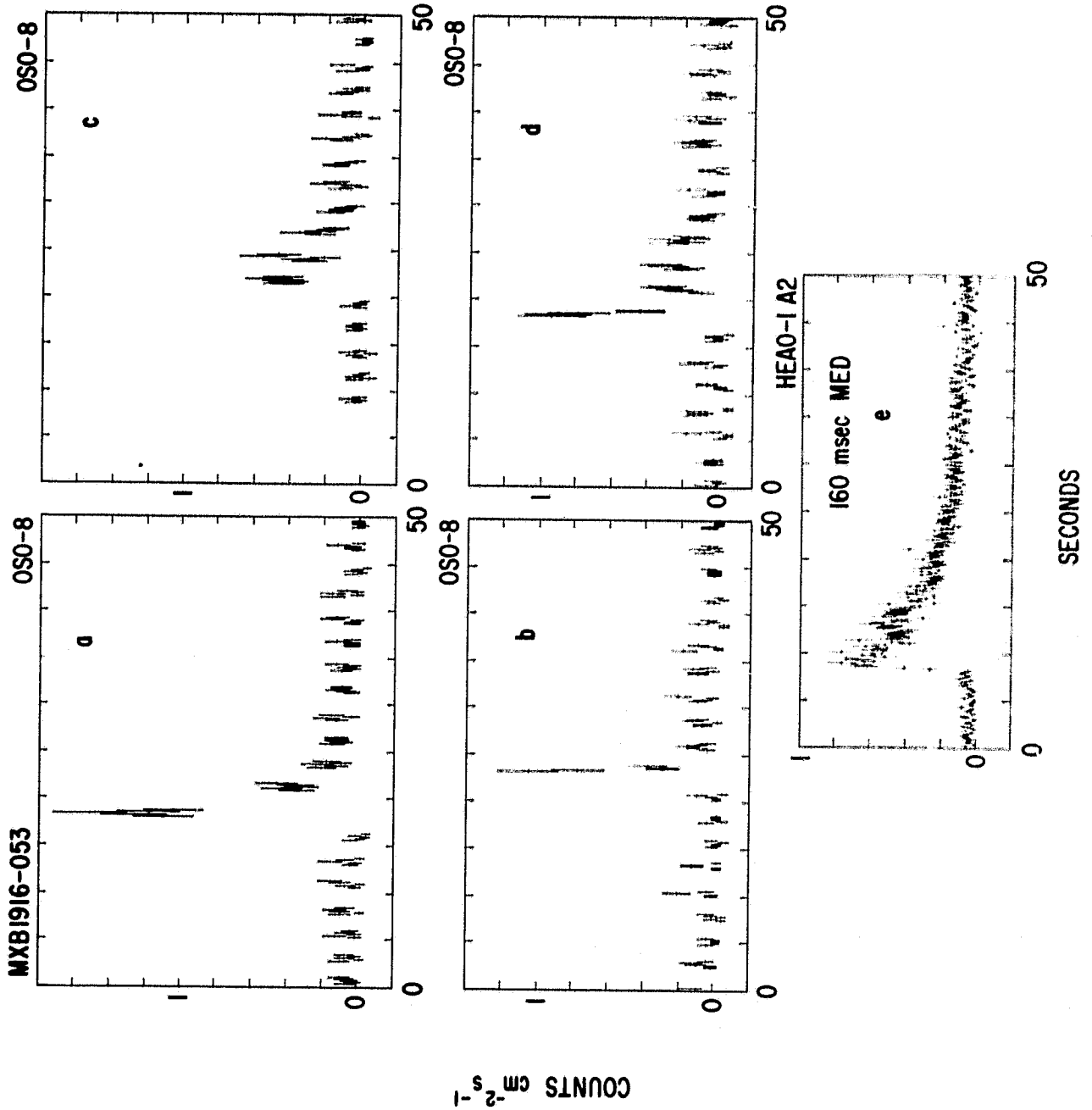
AVERAGE SPECTRA



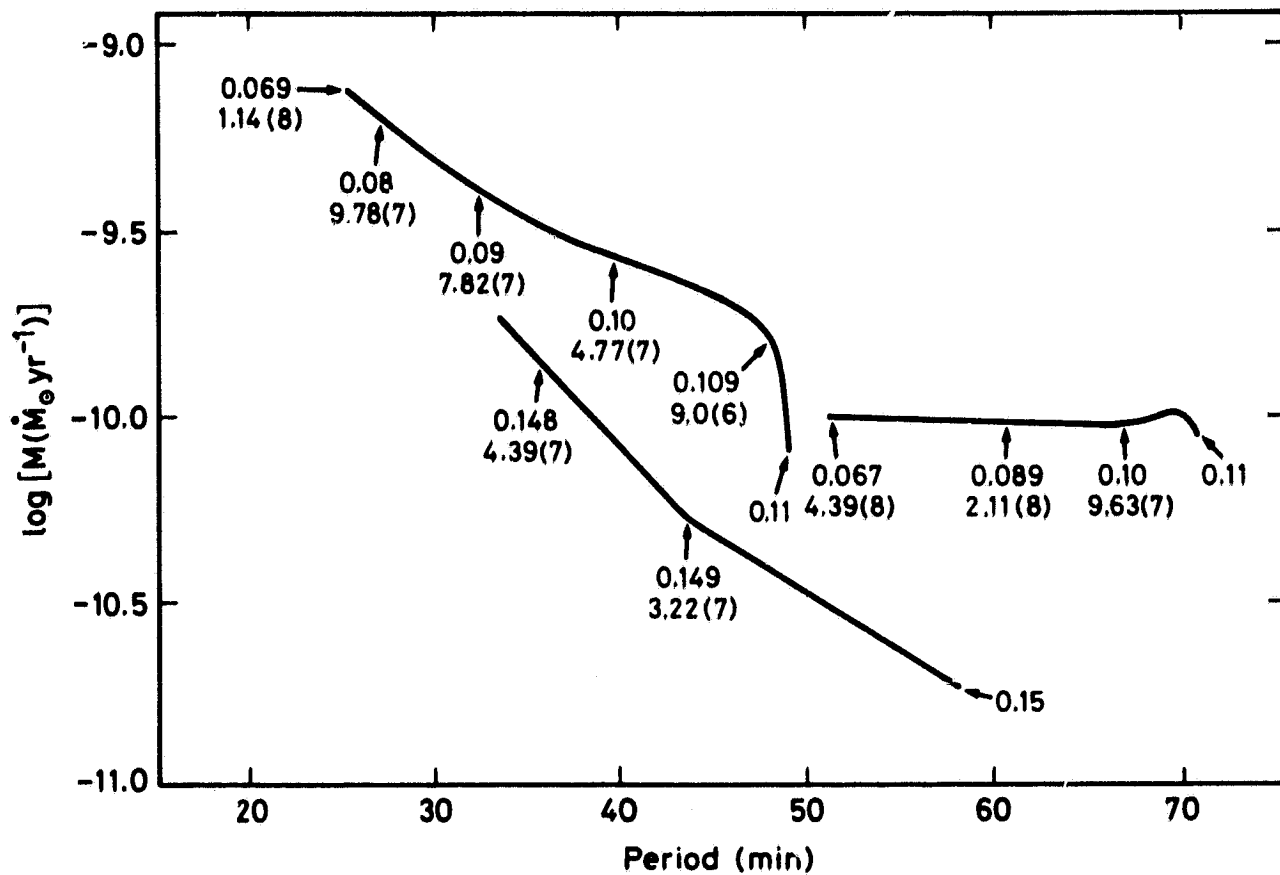
ORIGINAL PAGE IS
OF POOR QUALITY



ORIGINAL PAGE IS
OF POOR QUALITY



ORIGINAL PAGE IS
OF POOR QUALITY



ADDRESS OF AUTHORS

**J.H. SWANK, Code 661, Laboratory for High Energy Astrophysics, NASA/Goddard
Space Flight Center, Greenbelt, MD 20771**

**R.E. TAAM, Department of Physics and Astronomy, Northwestern University,
Dearborn Obs., Evanston, IL 60201**

N.E. WHITE, ESTEC, Postbus 299, 2200 AG Noordwijk Zh, THE NETHERLANDS